

# Effect of acrylic copolymer adsorption on the colloidal stability of a 3Y-TZP suspension

Yangqiao Liu, Lian Gao\*, Jing Sun

*State Key Lab on High Performance Ceramics and Superfine Microstructure, Shanghai Institute of Ceramics,  
Chinese Academy of Sciences, 1295 Dingxi Road, Shanghai 200050, PR China*

Received 21 March 2001; accepted 10 July 2001

## Abstract

This article investigates the adsorption of an acrylic acid/acrylate copolymer on 3Y-TZP and its influence on the stability of colloidal 3Y-TZP aqueous suspensions. Potentiometric titration shows that ionization degree of the copolymer increases from 0 at pH 2.5 to 1 at pH 9. The adsorption is characterized using the chemical oxygen demand (COD) method. The influences of pH, copolymer concentration and electrolyte concentration are investigated. The adsorption density is found to increase pronouncedly with increasing  $\text{KNO}_3$  concentration at higher pH, while is almost independent upon  $\text{KNO}_3$  concentration at lower pH. The zeta potential of Y-TZP decreases as a result of copolymer adsorption. The optimum copolymer concentration at pH 8.8 is around 2 dry mass base (dmb)%, determined by both effective diameter measurements and rheological characterization. The stabilization of the copolymer for the suspension is also evidenced by scanning electron microscopy (SEM) analysis of the sediments. The fractal dimensions of sediments obtained with and without dispersant were determined and compared using the limited fractal dimension method. © 2002 Elsevier Science Ltd. All rights reserved.

**Keywords:** Adsorption; Dispersant; Suspensions; TZP;  $\text{ZrO}_2$

## 1. Introduction

Dispersion of ceramic powders in aqueous suspensions is of special significance in the ceramic industry.<sup>1–4</sup> For instance, a stable powder suspension is a prerequisite for coating process, which is an important method for composite powder preparation.<sup>4</sup> In addition, stable suspensions with high solids loading are required for the colloidal forming of ceramics, which is believed to be a potential way to eliminate the structural defects and stress centres in the sintered product.<sup>1,2</sup>

Polymeric dispersants have been widely used to enhance the stability of the suspension. A considerable amount of work has been reported in the literature on the application of polyacrylic acid (PAA) and polymethacrylic acid (PMAA) as dispersants for ceramic powders and its adsorption characteristics on these substrates.<sup>1,5,6</sup> Vermöhlen et al.<sup>7</sup> have systematically investigated the influence of ionic strength, pH, molar mass, and  $\text{Ca}^{2+}$  ions

on the adsorption of PAA onto alumina. In recent years, copolymer polyelectrolytes have gained more and more attention due to its excellent dispersing abilities.<sup>8–10</sup> Kuo et al.<sup>8</sup> has reported the application of acrylic acid/methacrylate ester copolymer as a dispersant for titania suspension and found that compared with homopolyelectrolytes, the copolymer results in a stable suspension in a wider concentration range. Hidehiro et al.<sup>9</sup> has investigated the stabilising effect of acrylic acid/acrylate ester copolymer for  $\text{Al}_2\text{O}_3$  suspension using AFM and rheological measurements. It has been found that the copolymer with the optimum hydrophilic to hydrophobic ratio 3:7 would result in the maximum repulsive force and the minimum viscosity of the suspension. Pina et al.<sup>10</sup> investigated the adsorption of a hydrolysed styrene maleic anhydride (hSMA) copolymer onto titanium dioxide. However, there is a paucity of studies on both the adsorption of copolymer on ceramic powders and its stabilizing effect for the aqueous suspensions and the relationship between them.

In the present study, the adsorption of an acrylic acid/acrylate ester copolymer on 3Y-TZP was characterized using a chemical oxygen demand (COD) method. Many

\* Corresponding author. Tel.: +86-21-6251-2990 6321; fax: +86-021-6251-3903.

E-mail address: liangaoc@online.sh.cn (L. Gao).

techniques, such as zeta potential measurements, effective diameter analysis, scanning electron microscopy (SEM) observation and rheological properties were used to characterize the influence of this copolymer on the stability of aqueous Y-TZP suspension. A novel limited fractal dimension method was employed to analyse the relationship of suspension stability with the fractal dimension value of sediment.

## 2. Experimental

### 2.1. Materials

Yttria stabilized tetragonal zirconia polycrystal (3Y-TZP) powders (Shenzhen Nanbo Company, China) were used as the starting material. Their specific surface area was determined to be 28.7 m<sup>2</sup>/g using the Micromeritics ASAP 2010 Specific Surface Area Analyzer. The elemental analysis was conducted by X-ray fluorescence (Philips, PW-2400, semiquantify) and the results are shown in Table 1. The dispersant used in this study (Acumer2000, Rohm and Haas) was the 43 wt.% aqueous solution of an acrylic acid/acrylate ester copolymer (Mw = 4500 g/mol) and its molecular structure is shown in Fig. 1. Analytical grade HNO<sub>3</sub> and NaOH were used in this study to adjust the pH. All other chemicals in this study were analytical grade. Distilled water was used in this study.

### 2.2. Sample preparation

Suspensions were prepared by adding a specific amount of 3Y-TZP powder in the aqueous solution of the required amount of copolymer. KNO<sub>3</sub> was added to adjust the ionic strength. Suspension pH was initially adjusted to the desired value with 0.1 M HNO<sub>3</sub> or NaOH solution. The slurries were mixed using a mixer (Turbula, Maschinenfabrik, Basel, Switzerland) for 24 h. After mixing, the pH of the suspension was measured again. The pH change after adsorption was within the

range of ±0.1 units. The milled suspension was used in the following characterization experiments. The mass concentration of the suspension for zeta potential analysis, effective diameter measurements, adsorption studies and SEM investigation was 2 and 60 wt.% for the rheological experiments.

### 2.3. Methods

Potentiometric titration was used to characterize the acid-base properties of the copolymer as a function of pH. A 5 g/l copolymer solution (20 ml) was acidified to pH 2.2 with HNO<sub>3</sub>. The sample was titrated with 0.1 M carbonate-free standard NaOH solution to a pH of 11.0. An identical titration was performed on a blank solution without copolymer. KON<sub>3</sub> was used to adjust the ionic strength. After correcting for volumetric changes due to dilution by the titrant, the titration curves were fit using a regression routine with an eighth-order polynomial equation. The regression correlation coefficient, *r*<sup>2</sup>, was > 0.999 in all cases. Using the regression data, the blank titration curve was then subtracted from the sample curve to obtain the net uptake of hydroxyl (OH<sup>−</sup>) ions as a function of pH.

A Zeta potential analyzer (Zetaplus, Brookhaven Instruments, Holtsville, NY) was used to measure the zeta potential of the 3Y-TZP particles in the aqueous suspension by electrophoresis. The zeta potential analysis for the 3Y-TZP suspension without dispersants were conducted on a 0.01 vol.% suspension. The mixture was ultrasonicated for 15 min prior to measurements. The suspension for the analysis with dispersants was prepared as follows: The milled suspension was centrifuged at 6000 rpm for 1 h. Then, a small drop of the suspension was dispersed in large amount of supernatant. An average of at least four measurements for each sample was reported. This dilute suspension was also used for the effective diameter measurements by light scattering method on Zetaplus Analyzer.

The amount of copolymer adsorbed by the 3Y-TZP was calculated by detracting the amount in the supernatant from the initial added amount. Copolymer concentration in the supernatant was determined using a chemical oxygen demand (COD) method.<sup>14</sup> The copolymer in this study could be oxidized by dichromate (K<sub>2</sub>Cr<sub>2</sub>O<sub>7</sub>) and the amount of copolymer was proportional to the amount of dichromate consumed. The detailed procedures were as follows: 20 ml test solution, 10 ml 0.25 M dichromate solution and 30 ml of concentrated H<sub>2</sub>SO<sub>4</sub> were mixed in a 150-ml beaker. 0.25 g Ag<sub>2</sub>SO<sub>4</sub> was then added as a catalyst. The mixture was boiled for 2 h. Preliminary experiments indicated that 2 h were enough for complete reaction. Then, the residual amount of dichromate was determined by titration using 0.1 M (NH<sub>4</sub>)<sub>2</sub>Fe(SO<sub>4</sub>)<sub>2</sub> solution. Blank experiments were carried out by titrating 10 ml copolymer-free dichromate

Table 1  
X-ray fluorescence results of 3Y-TZP powder (semiquantify)

Component	ZrO <sub>2</sub>	Y <sub>2</sub> O <sub>3</sub>	HfO <sub>2</sub>	SiO <sub>2</sub>	SO <sub>3</sub>	Cl	Fe <sub>2</sub> O <sub>3</sub>	NiO	ZnO
Content (wt.%)	93.6	1.9	1.8	0.29	0.16	0.13	0.12	0.09	0.03

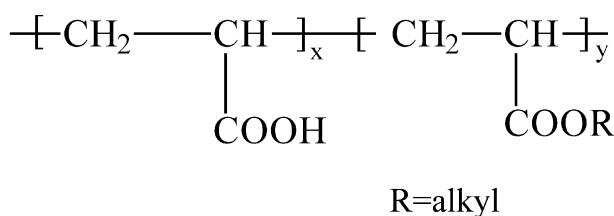


Fig. 1. Molecular structure of the copolymer used in this study.

solution. The COD value of the copolymer solution was calculated according to the following equation:<sup>11</sup>

$$COD = \frac{c(V_1 - V_2) \times 8000}{V_0}$$

where *COD* (mg/l) is the chemical oxygen demand value; *c* (mol/l) the concentration of (NH<sub>4</sub>)<sub>2</sub>Fe(SO<sub>4</sub>)<sub>2</sub> solution; *V*<sub>1</sub> (ml) volume of (NH<sub>4</sub>)<sub>2</sub>Fe(SO<sub>4</sub>)<sub>2</sub> solution used for titrating the residual dichromate after boiling with the test solution; *V*<sub>2</sub> (ml) the volume of (NH<sub>4</sub>)<sub>2</sub>Fe(SO<sub>4</sub>)<sub>2</sub> solution consumed in the blank experiment; *V*<sub>0</sub> (ml) is the volume of test copolymer solution. The COD value of the standard 100 mg/l copolymer solution was determined using the same method. The copolymer concentration in the supernatant was thus calculated according that the copolymer concentration was proportional to the COD value. COD analyses were performed in duplicate and the yielding experimental error was no more than 5%. The supernatant was diluted before analysis to insure the final concentration was in the range of 10–700 mg/l.

The milled suspensions were allowed to settle on a copper pellet under gravity until a thin sediment film was formed. Then the sediment was dried in the air and observed with a scanning auger microscope (SAM) (Microlab-310F, VG Scientific Ltd). To obtain high-quality micrographs, the sediments were coated with a thin gold layer prior to measurement.

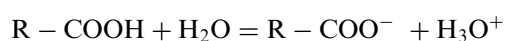
The rheological measurements were carried out using a rotary viscometer (Rheomat Mettler 260, Switzerland). Before performing rheological characterization, the samples were presheared at 500 s<sup>−1</sup> for 2 min followed by at least 2 min rest period in order to provide a common and consistent shear history for the systems. All the experiments were carried out at 25 °C. Shear rate increased from 0.01 to 200 s<sup>−1</sup>. Data, including shear stress and shear rate were collected five times after getting stable data and averaged in a dedicated computer.

### 3. Results and discussion

#### 3.1. Charge behavior of the copolymer and the powder

The interaction between the copolymer and the powder varies a lot at different pH values, upon which the charge behavior of both the dispersant and the powder depends. Thus, the dissociation of the copolymer and the electrokinetic behavior of the powder were determined prior to the adsorption studies.

In comparison to the inertness of the ester groups, the carboxylic groups in the chain of the copolymer can dissociate in the aqueous solution.



$$K_a = \frac{[R - COOH^-][H_3O^+]}{[R - COOH]}$$

$$pK_{app} = -\log K_a = pH - \log\left(\frac{\alpha}{1-\alpha}\right)$$

where  $\alpha$  is the fraction of dissociated carboxyl groups,  $pK_{app}$  is the apparent dissociation constant of the poly-electrolyte. The degree of ionization for copolymer was calculated from the net uptake of hydroxyl ions and is shown as a function of pH in Fig. 2. The curves show that the dissociation degree  $\alpha$  increases from 0 at pH below 2.5 to  $\approx 1$  above pH 9. In comparison to the dissociation reported for PAA (*Mr* = 5000)<sup>5</sup> and PMAA (*Mr* = 8000–10,000),<sup>12</sup> the acrylic acid/acrylate ester copolymer in this study has a higher degree of dissociation at a given pH. This can be interpreted as follows: In comparison to the monoprotic acids, the dissociation of each carboxyl group along the polyelectrolyte chain significantly affects the ionization of neighbouring groups. Dissociation becomes increasingly difficult as the fraction of ionized sites,  $\alpha$ , increases as a consequence of

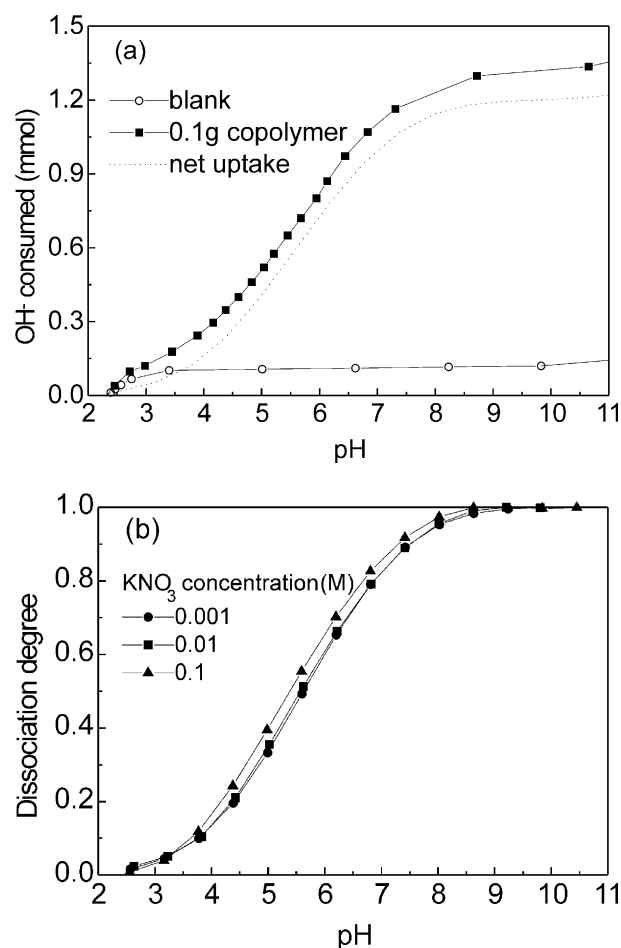


Fig. 2. Acid-base potentiometric titration of the acrylic copolymer: (a) titration curves in 0.001 M KNO<sub>3</sub> solution showing the net uptake of hydroxide ions by the copolymer and (b) the calculated degree of ionization of the copolymer, both as a function of solution pH.

electrostatic interactions. However, the electrostatic repulsion between the negatively charged carboxylates of the copolymer is reduced by the presence of the neutral ester groups, leading to an easier dissociation of the copolymer than PAA or PMAA at the same dissociation degree. It can also be seen from Fig. 2 that the ionization degree of the copolymer in 0.1 M  $\text{KNO}_3$  is slightly higher than that in 0.01 or 0.001 M  $\text{KNO}_3$  solutions. The increase in the electrolyte concentration results in a more effective electrostatic shielding of the ionized acid groups and makes the dissociation of other acid groups less difficult,  $\alpha$  increases.

Fig. 3 illustrates the zeta potentials of 3Y-TZP powders as a function of pH for different  $\text{KNO}_3$  concentrations. The 3Y-TZP powder has a native isoelectric point ( $\text{pH}_{\text{IEP}}$ ) at  $\text{pH} \sim 6.4$ , similar to the value reported in literature.<sup>13,14</sup> The zeta potential curve of the bare Y-TZP is parallel by the IEP, behavior when no specific ion adsorption occurs. The absolute value of zeta potentials in 0.1 M  $\text{KNO}_3$  is much lower than that in 0.001 or 0.01 M  $\text{KNO}_3$ . This is due to the compression of the double layer as a result of the increased electrolyte concentration.

### 3.2. Adsorption studies

Considering the charging behavior of the 3Y-TZP and the copolymer in aqueous electrolyte solution, three particular pH values are chosen for the adsorption study: (1)  $\text{pH} = 3.3$ , where the 3Y-TZP is net positively charged while the copolymer is almost uncharged ( $\alpha = 5\%$ ); (2)  $\text{pH} = 6.4$ , where the 3Y-TZP is uncharged while the copolymer is about 70% ionized; (3)  $\text{pH} = 8.8$ , where the 3Y-TZP is net negatively charged while the copolymer is almost fully ionized.

Fig. 4 shows the adsorption in 0.001 M  $\text{KNO}_3$  at the three pH values, plotted as milligrams of copolymer adsorbed per square meter of surface area of 3Y-TZP versus the initial amount of copolymer added (on a dry

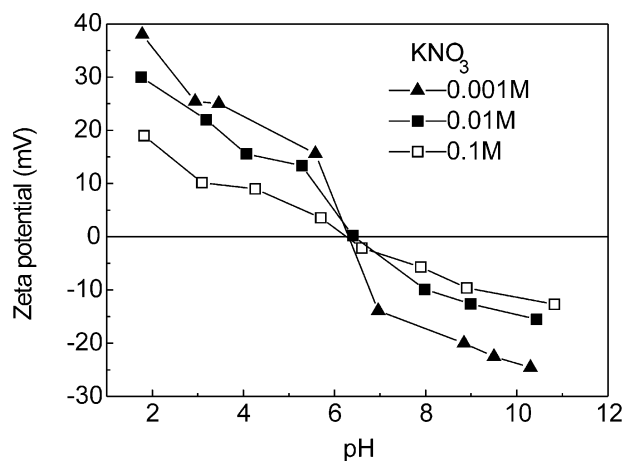


Fig. 3. The  $\zeta$  potential of 3Y-TZP suspension at different  $\text{KNO}_3$  concentrations as a function of pH.

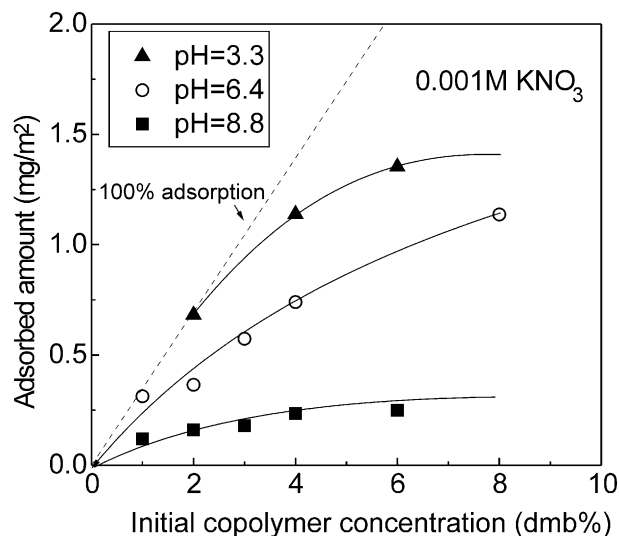


Fig. 4. Adsorbed amount of copolymer on 3Y-TZP, plotted as a function of the initial copolymer concentration in 0.001 M  $\text{KNO}_3$  solution at different pH values.

mass of 3Y-TZP basis). The dash diagonal line represents the adsorption behavior that would occur if 100% of the copolymer added were to adsorb. For all the pH values investigated, the adsorbed amount increases with increasing copolymer concentration, followed by a weakly increasing isotherm at elevated copolymer concentration. The isotherm at pH 3.3 is of high-affinity characteristics, evidenced by the sharp increase of the adsorbed amount at low copolymer concentrations. The isotherm at pH 8.8 is of low-affinity since significant amount of copolymer remains unadsorbed even at low initial copolymer concentration. The affinity of the adsorption isotherm at pH 6.4 is higher than that at pH 8.8 but lower than that at pH 3.3. In addition to the affinity, the adsorbed amount also increases with decreasing pH. The pH dependence that is observed here is similar to previously reported data for the adsorption of PAA on alumina,<sup>1,15</sup> silicon nitride,<sup>5</sup> anatase and zirconia.<sup>16</sup> The decrease in the adsorption amount may be explained taking into consideration the surface charge of the powder as well as the ionization degree of the copolymer, both of which are dependent on pH. At low pH values, the COOH group of the acrylic-based polyelectrolytes can act as a proton donor or acceptor, and thus adsorption may take place by hydrogen bonding between the hydroxylated 3Y-TZP surface and the carboxyl groups of the copolymer. Similar mechanism has been proposed by Santhiya et al.,<sup>15</sup> based on the results of FTIR analysis for PAA adsorption on alumina. An additional contribution to the adsorption affinity may result from hydrophobic forces between the copolymer and the aqueous solution, which increase in importance as  $\alpha$  decreases in acidic media. Hydrophobic interactions would have a tendency to drive the polymer onto the particle surface to reduce the free energy that is

associated with the structuring of water molecules around the hydrophobic polymer.<sup>12</sup> In the weak acidic range below  $\text{pH}_{\text{iep}}$ , the adsorption is enhanced due to the electrostatic interaction between the oppositely charged copolymer and the powder. For high pH values, the adsorption of copolymer is hampered by the electrostatic repulsion between the both negatively charged copolymer and the powder, thus adsorption can only take place via chemical interaction and hydrogen bonding in this case. The fact that at pH 8.8, where the copolymer and the powder are both negatively charged, a substantial adsorption is observed indicates that specific interactions are present. In addition, the configuration of the adsorbed polyelectrolytes also changes a lot for different pH values. At pH 3.3, the copolymer behaves like a neutral polymer and the formation of loops in the adsorbed configuration is enhanced, which permits a dense packing on the particle surface.<sup>1,5</sup> Under alkaline conditions, the electrostatic repulsion between the ionized groups on the copolymer makes the chain more stretched, lowering the adsorbed amount. The increase in the hydrodynamic size of polyelectrolytes at high pH also explains this decrease.<sup>6</sup>

To determine the monolayer adsorption of the copolymer quantitatively, the data in Fig. 4 are analyzed using the Langmuir monolayer adsorption equation:<sup>6</sup>

$$\frac{C_{\text{eq}}}{A_s} = \frac{C_{\text{eq}}}{A_{\text{max}}} + \frac{k}{A_{\text{max}}}$$

The data are plotted as  $C_{\text{eq}}/A_s$  versus  $C_{\text{eq}}$  in Fig. 5, where  $C_{\text{eq}}$  (mg/l) is the equilibrium concentration of adsorbate in solution,  $A_s$  (mg/m<sup>2</sup>) the adsorbed amount for a given equilibrium concentration and  $A_{\text{max}}$  (mg/m<sup>2</sup>) the monolayer adsorption per unit solid surface;  $k$  is a constant. Straight lines are observed, indicating that adsorption follows Langmuir monolayer-type. The slopes of the straight lines represent the reciprocal of the

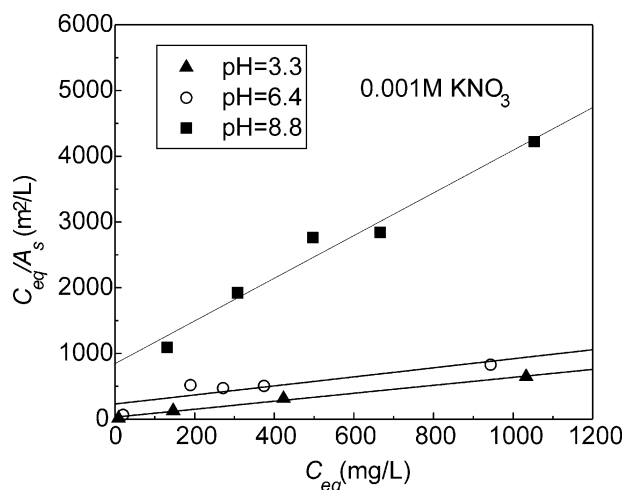


Fig. 5. Replot of Fig. 4, based on the Langmuir equation.

monolayer adsorption of dispersants ( $1/A_{\text{max}}$ ). The values of  $A_{\text{max}}$  calculated from Fig. 5 are 1.65, 1.45 and 0.28 mg/m<sup>2</sup> for pH 3.3, 6.4 and 8.8, respectively.

Fig. 6 shows the variation of adsorbed amount as a function of  $\text{KNO}_3$  concentration for an initial copolymer concentration of 5 dry mass base (dmb)%. It can be found that the adsorbed amount is roughly independent upon electrolyte concentration at pH 3.3, however, increases markedly with increasing electrolyte concentration at pH 8.8. At pH 3.3, the adsorption occurs mainly by hydrogen bonding and contribution from the electrostatic attraction is negligible due to the low ionization degree of the copolymer. Thus, the adsorption amount is only determined upon the number of hydrogen bonding sites of the powder, while independent upon the electrostatic status. Changes in the inert electrolyte concentration will have no influence on the adsorption amount at this pH. The increase in the adsorbed amount with increasing electrolyte concentration at alkaline region has been reported for the adsorption of PAA onto alumina<sup>7</sup> and humic acid onto hematite.<sup>17</sup> This occurs because the background salt has an electrostatic shielding effect on the negatively charged  $\text{COO}^-$  sites on the copolymer chain, thereby causing the chains to behave like uncharged polymers and enhancing the development of loops. In addition, the salts also screen the electrostatic repulsion between ionized copolymer and Y-TZP powder, contributing to the increase in the adsorbed amount.

### 3.3. Electrokinetic properties of Y-TZP powder

Fig. 7 shows zeta potential measurements of 3Y-TZP suspensions in 0.001 M  $\text{KNO}_3$  at different pH values as a function of the initial copolymer concentration. For all pH values investigated, the zeta potential initially

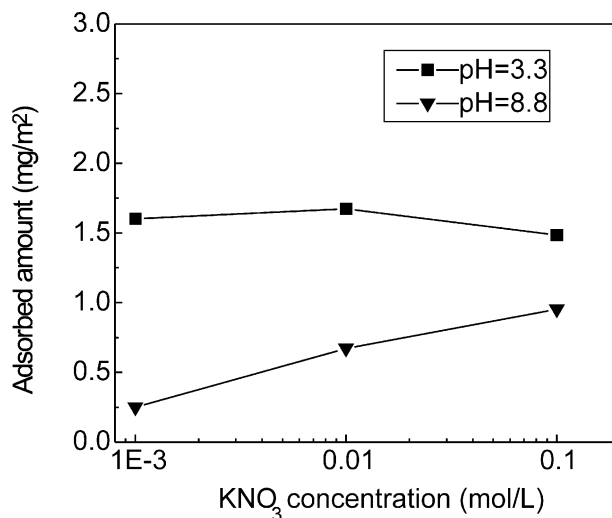


Fig. 6. Adsorbed amount of copolymer on 3Y-TZP as a function of  $\text{KNO}_3$  concentration for an initial copolymer concentration of 5 dmb%.

shows a continuous decrease, followed by a constant value with increasing copolymer concentration. The constant value of the zeta potential is  $-25$ ,  $-40$  and  $-45$ , respectively, for pH 3.3, 6.4 and 8.8. At pH 3.3, where the copolymer in the solution is almost uncharged, the adsorption of copolymers also causes a significant decrease in the zeta potential. This is because the segmental dissociation constant is influenced by the local electrostatic potential near the surface. Segments can adjust their ionization to compensate or screen the surface charge.<sup>18</sup> The modification of the zeta potential by adsorbed polyelectrolytes at pH where the bulk polyelectrolytes are uncharged has been reported for PAA on silicon nitride by Hackley<sup>5</sup> and PMAA and humic acid on alumina.<sup>17</sup> The zeta potential decrease resulting from copolymer adsorption is still obvious at  $\text{pH} > \text{pH}_{\text{iep}}$ , where electrostatic repulsion exists between copolymer and powder surface. This behavior is indicative of a chemical contribution to the free energy of adsorption to overcome adsorption barriers caused by electrostatic repulsion.<sup>1</sup> Comparing Figs. 3 and 7, it can be seen that the zeta potential curve is not consistent with the adsorption trends since the adsorption amount increases continuously in the experimental concentration range and no adsorption saturation is observed. From this result, it can be assumed that the initial decrease in zeta potential is due to the adsorption of the negatively charged copolymer. At higher copolymer concentrations, the adsorption of the copolymer increases the charge of the particle but is offset by the decrease in zeta potential induced by the higher electrolyte concentration generated by the polyelectrolyte. Similar behavior has also been reported by Pina et al.<sup>9</sup> for the adsorption of a hydrolysed styrene maleic anhydride copolymer on titania.

Fig. 8 shows the variation of the zeta potential as a function of the adsorbed amount in 0.001 M  $\text{KNO}_3$ . The data have been taken from Figs. 4 and 7. For all

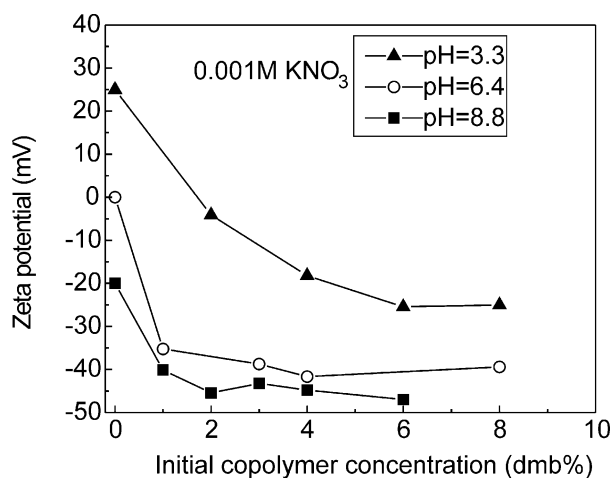


Fig. 7. The  $\zeta$  potential of 3Y-TZP suspension in 0.001 M  $\text{KNO}_3$  vs. initial copolymer concentration at different pH values.

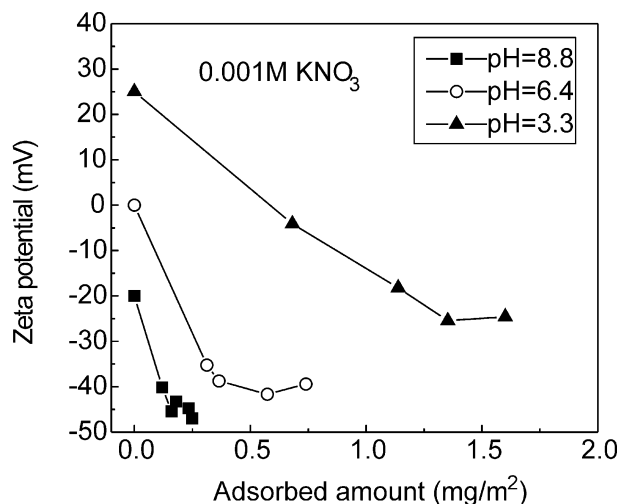


Fig. 8. The  $\zeta$  potential of 3Y-TZP suspension in 0.001 M  $\text{KNO}_3$  vs. the adsorbed amount at different pH values.

pH values investigated, the zeta potential initially decreases linearly, followed by a constant value at higher adsorbed amount. The linear dependency of zeta potential on the adsorbed amount indicates that the copolymer is the surface-charge-determining species. The slope of the curves, representing the capability of the copolymer to modify the surface charge at different pH values, increases with increasing pH. This is consistent with the increased dissociation degree of copolymer at high pH values. The total zeta potential decrease at pH 3.3, 6.4 and 8.8 is 50, 40, 25 mV, respectively, which is obtained at the adsorbed amount of 1.35, 0.37 and 0.18  $\text{mg/m}^2$ . Considering the net zeta potential decrease at a given pH is only induced by the dissociated segments of the adsorbed copolymer, it should be proportional to the product of adsorbed amount and  $\alpha$  of the adsorbed copolymer. Since the powder carries no charge at pH 6.4, we can assume that the dissociation of the copolymer adsorbed at this pH is not affected by the local electric potential and is identical to the dissociation degree in the bulk solution ( $=70\%$ ). The calculated  $\alpha$  for the adsorbed copolymer was 24 and 90% for pH 3.3 and 8.8, respectively. This means that the dissociation degree of the adsorbed segments is higher than in the bulk solution at low pH, while, slightly lower than in the bulk solution at high pH. This agrees well with the dissociation behavior of the adsorbed weak polyelectrolytes predicted by Bohmer et al.<sup>18</sup>

### 3.4. Effect of copolymer on the dispersion properties

Stable suspensions of ceramic powders with anionic polyelectrolytes are often prepared under alkaline conditions.<sup>1,5</sup> The high absolute values of zeta potential at pH 8.8 also show this (Fig. 7). Thus, the suspension properties were evaluated at pH 8.8 in this study. Fig. 9 shows the variation of effective diameter of Y-TZP suspension as a

function of initial copolymer concentration at pH 8.8. Also shown is the zeta potential curve under identical conditions. The effective diameter decreases monotonically with increasing copolymer concentration. The effective diameter reaches a constant value of  $\sim 200\text{nm}$  when the initial copolymer concentration is higher than 2 dmb%. This value is identical to the minimum amount of dispersant for constant zeta potential (Fig. 7), although the adsorption saturation has not been achieved (Fig. 4).

The dispersing effect of the copolymer is also verified by comparing the SEM micrographs of sediments resulting from 2 wt.% suspensions at pH 8.8 without and with 2 dmb% copolymer (Fig. 10). Large differences can be observed when comparing Fig. 10(a) and (b). Large flocs are observed in the sediments of suspensions without copolymer, while, particles of the sediments with 2 dmb% copolymer are not associated with one another, confirming that particles are well dispersed in the suspension.

The box-dimension method for fractal dimension determination was first proposed by Yang et al. to evaluate the effect of antifoulant in circulating water system.<sup>19</sup> This method was used in the previous study to show the relationship between the suspension stability and the sediment fractal dimension.<sup>3</sup> The results show that the more stable the suspension, the higher the fractal dimension of the sediment.

According to the fractal dimension definition<sup>20,21</sup>

$$D = \lim_{\varepsilon \rightarrow 0} \frac{\ln N(\varepsilon)}{\ln \frac{1}{\varepsilon}}$$

where  $\varepsilon$  is the measurement scale,  $N(\varepsilon)$  is the measurable property using  $\varepsilon$ . For the measurement of  $D$  for the sediment surface through digital imaging by the box-dimension method,<sup>3</sup> the above equation can be re-written as<sup>22</sup>

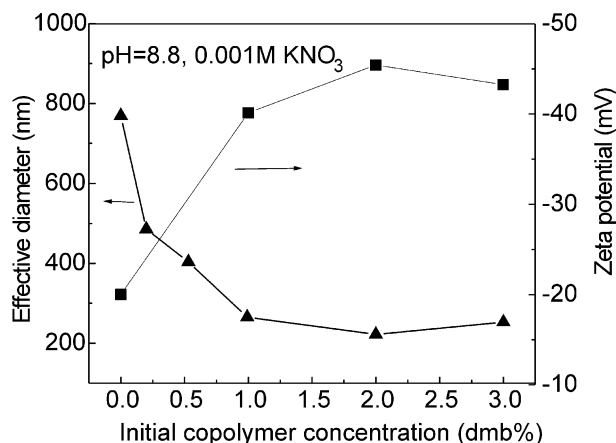


Fig. 9. Effective diameter and  $\zeta$  potential of 3Y-TZP particles in 0.001 M  $\text{KNO}_3$  at pH 8.8, as a function of the initial copolymer concentration.

$$D = \lim_{n \rightarrow \infty} \frac{\ln \sum_{i=0}^{n-1} \sum_{j=0}^{n-1} B_{ij}}{\ln n}$$

where  $n = 1/\varepsilon$ ,  $n$  is the length of the side of the cubic box. In the present work,  $n = 64, 128, 256, 512, 1024, 2048, 4096$  and  $8192$ . For each value of  $n$ , there will be a corresponding value of  $D$  according to Eq. (5). Owing to the processing capability limit of the computer, a further larger value of  $n$  was not adopted. By non-linear regression, the limit value of  $D$  was obtained, as shown in Fig. 11. It can be seen that the fractal dimension  $D$  for

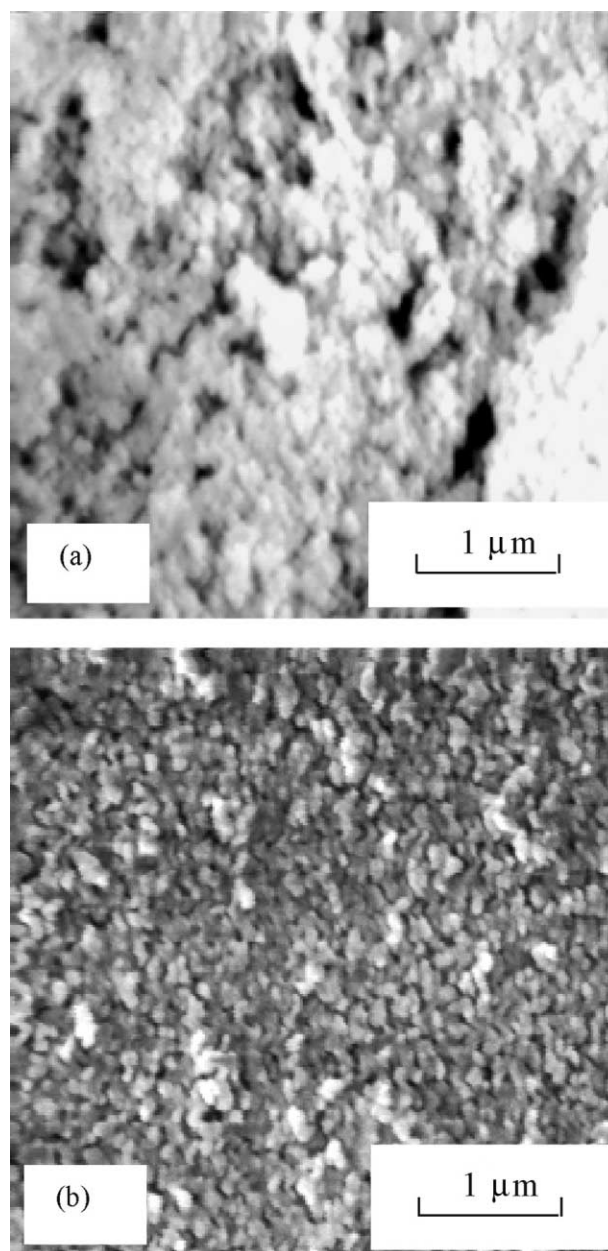


Fig. 10. SEM micrographs of sediments resulting from 2 wt.% 3Y-TZP suspensions with 0.001 M  $\text{KNO}_3$  at pH 8.8 (a) without dispersants (b) with 2 dmb% copolymer.

sediment with 2 wt.% copolymer is higher than that for sediment without dispersant. This is in accordance with the result obtained in the previous work,<sup>3</sup> but the result obtained in the present paper is more reasonable. This is because the fractal dimension value changes with  $n$  for the smaller values of  $n$ , as can be seen clearly from Fig. 10.

Fig. 12 shows the plot of apparent viscosity of 60 wt.% 3Y-TZP suspension with the shear rate for different copolymer concentrations. Suspensions of the same mass fraction can not flow without dispersants and can not be used to measure the viscosity. The addition of copolymer dramatically reduces the viscosity of the suspension. The viscosity minimum occurs in the copolymer concentration range of 1.7–2.5 dmb%. Once the copolymer concentration is higher than 2.5 dmb%, the suspension viscosity significantly increases. The optimum copolymer concentration determined by the rheological measurements coincides with that determined from the zeta potential and the effective diameter measurements for comparatively dilute suspensions. This is consistent with the result obtained by Fagerholm et al.<sup>23</sup>

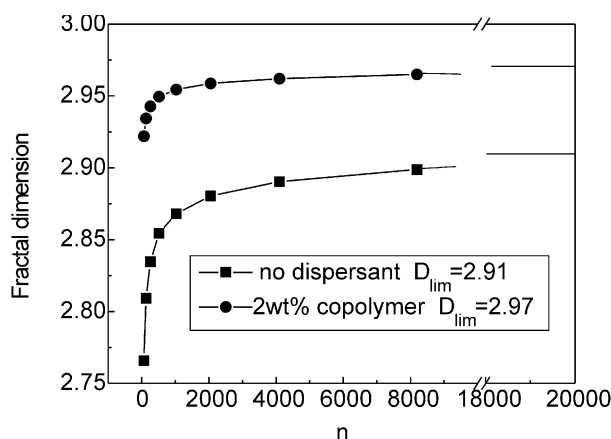


Fig. 11. Limited fractal dimension values of sediments in Fig. 10.

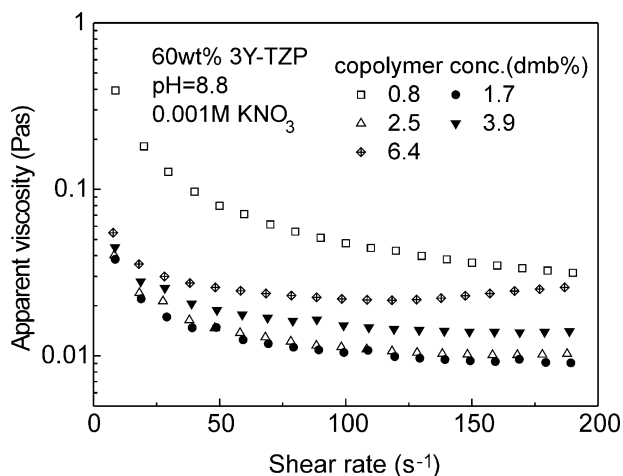


Fig. 12. Apparent viscosity of 60 wt.% 3Y-TZP aqueous suspensions as a function of the shear rate, at the  $\text{KNO}_3$  concentration of 0.001 M and pH 8.8.

that the optimum copolymer dosage is independent upon the solid loading. The excess amount of dispersant is detrimental to stabilization.<sup>5</sup> The unadsorbed copolymer in the suspension reduces the electrostatic repulsion between particles due to the screening effect of the increased ions. This effect becomes increasingly important at higher copolymer concentrations, causing an increase in the viscosity with increasing copolymer dosage.

The stabilization mechanism of polyelectrolytes in alkaline media is proposed to be electrosteric mechanism.<sup>1</sup> The decrease of the zeta potential of 3Y-TZP from  $-20$  to  $-45$  mV in the presence of 2 dmb% copolymer at pH 8.8 indicates that adsorbed copolymer increases the electrostatic repulsion between the powders. Thus, electrostatic repulsion can be considered as a contribution to the stabilization of the suspension by the copolymer. In addition, in comparison to the flat conformation of PAA at alkaline conditions, the copolymer can form the structure of loops and tails since the adsorbed sites in polymer chain is reduced by the presence of hydrophilic groups.<sup>10</sup> The presence of the ester groups also reduces the electrostatic repulsion between the dissociated carboxyl sites, making the formation of loops and tails easier. This steric effect resulting from the protruding loops and tails, combined with the electrostatic repulsion, enhances the stability of the suspension.

#### 4. Conclusion

The adsorption density of an acrylic copolymer on Y-TZP powder increases with increasing copolymer concentration and decreasing pH. The increase in inert electrolyte concentration causes a significant increase in adsorption density at higher pH, while almost had no effect upon adsorption density at lower pH. The copolymer is the potential-determining species and results in a decrease in the zeta potential of 3Y-TZP in the whole pH range studied. The addition of copolymer enhances the stability of the 3Y-TZP suspension significantly at pH 8.8. The optimum copolymer concentration determined by particle size analysis and rheological measurements is 2 dmb%. The limited fractal dimension analysis show that the addition of 2 wt.% copolymer results in a higher fractal dimension value than that without dispersant. The stabilization effect of the copolymer under alkaline condition is attributed to the electrosteric mechanism.

#### Acknowledgements

This work was funded by the State Key Lab of High Performance and Superfine Microstructures (No. 233500). Professor L. Yu is kindly acknowledged for taking the AES micrographs.



## References

1. Cesarano, J. III. and Aksay, I. A., Stability of aqueous  $\alpha$ -Al<sub>2</sub>O<sub>3</sub> suspensions with poly(methacrylic acid) polyelectrolyte. *J. Am. Ceram. Soc.*, 1988, **71**, 250–255.
2. Sigmund, W. M., Bell, N. S. and Bergstrom, L., Novel powder-processing methods for advanced ceramics. *J. Am. Ceram. Soc.*, 2000, **83**, 1557–1574.
3. Liu, Y. Q., Gao, L., Yu, L. and Guo, J. K., Adsorption of PBTCA on alumina surfaces and its influence on the fractal characteristics of sediments. *J. Colloid and Interface Sci.*, 2000, **227**, 164–170.
4. Gao, L., Wang, H. Z., Hong, J. S., Miyamoto, H., Miyamoto, K., Nishikawa, Y. and Torre, S. D. D. L., SiC-ZrO<sub>2</sub>(3Y)-Al<sub>2</sub>O<sub>3</sub> nanocomposites superfast densified by spark plasma sintering. *Nanostruct. Mater.*, 1999, **11**, 43–49.
5. Hackley, V. A., Colloidal processing of silicon nitride with poly(acrylic acid): 1, adsorption and electrostatic interactions. *J. Am. Ceram. Soc.*, 1997, **80**, 2315–2325.
6. Jean, J. H. and Wang, H. R., Dispersion of aqueous barium titanate suspensions with ammonium salt of poly(methacrylic acid). *J. Am. Ceram. Soc.*, 1998, **81**, 1589–1599.
7. Vermöhlen, K., Lewandowski, H., Narres, H.-D. and Schwuger, M. J., Adsorption of polyelectrolytes on oxide—the influence of ionic strength, molar mass, and Ca<sup>2+</sup> ions. *Colloids and Surfaces A*, 2000, **163**, 45–53.
8. Kuo, P. L., Chang, T. C. and Lu, L. M., Functional polymers for colloidal applications. 1. Structural effects of lipophile-modified polyacrylates on adsorption and dispersion ability. *J. Appl. Polym. Sci.*, 1992, **44**, 859–867.
9. Pina, A., Nakache, E., Feret, Bruno and Depraetere, P., Copolymer polyelectrolyte adsorption onto titanium dioxide. *Colloids and Surfaces A*, 1999, **158**, 375–384.
10. Kamiya, H., Fukuda, Y., Suzuki, Y. and Tsukada, M., Effect of polymer dispersant structure on electrosteric interaction and dense alumina suspension behavior. *J. Am. Ceram. Soc.*, 1999, **82**, 3407–3412.
11. Anon. Water Determination—Determination of the Chemical Oxygen Demand—Dichromate Method. National Standards of the People's Republic of China, GB11914-89.
12. Paik, U., Hackley, V. A. and Lee, H. W., Dispersant-binder interaction in aqueous silicon nitride suspensions. *J. Am. Ceram. Soc.*, 1999, **82**, 833–840.
13. Biggs, S., Scales, P. J., Leong, Y. K. and Healy, T. W., Effects of citrate adsorption on the interactions between zirconia surfaces. *J. Chem. Soc. Faraday Trans.*, 1995, **91**, 2921–2928.
14. Sun, J., Gao, L. and Guo, J. K., Influence of the initial pH on the adsorption behavior of dispersant on nano zirconia powder. *J. Eur. Ceram. Soc.*, 1999, **19**, 1725–1730.
15. Santhiya, D., Subramanian, S., Natarajan, K. A. and Mlgham, S. G., Surface chemical studies on the competitive adsorption of poly(acrylic acid) and poly(vinyl alcohol) onto alumina. *J. Colloid Interface Sci.*, 1999, **216**, 143–153.
16. Vedula, R. R. and Spencer, H. G., Adsorption of poly(acrylic acid) of titania(anatase) and zirconia colloids. *Colloids and Surfaces. A*, 1991, **58**, 99–110.
17. Vermeer, A. W. P., Riemsdijk, W. H. and Koopal, L. K., Adsorption of humic acid to mineral particles. 1. Specific and electrostatic interactions. *Langmuir*, 1998, **14**, 2810–2819.
18. Blaakmeer, J., Bohmer, M. R., Stuart, M. A. C. and Fleer, G. J., Adsorption of weak polyelectrolytes on highly charged surfaces. Poly(acrylic acid) on polystyrene latex with strong cationic groups. *Macromolecules*, 1990, **23**, 2301–2309.
19. Yang, Q. F., Ding, J. and Shen, Z. Q., Investigation on fouling behaviors of low-energy surface and fouling fractal characteristics. *Chem. Eng. Sci.*, 2000, **55**, 797–805.
20. Mandelbrot, B. B., *Fractal: Form, Chance and Dimension*. Freeman, New York, 1977.
21. Mandelbrot, B. B., *The Fractal Geometry of Nature*. Freeman, New York, 1982.
22. Yang, Q. F., Ding, J. and Shen, Z. Q., Investigation of calcium carbonate scaling on ELP surface. *J. Chem. Eng. Jpn.*, 2000, **33**, 591–596.
23. Fagerholm, H. B., Mikkola, P., Rosenholm, J. B., Liden, E. and Carlsson, R., The influence of lignosulphonate on the properties of single and mixed Si<sub>3</sub>N<sub>4</sub> and ZrO<sub>2</sub> suspensions. *J. Eur. Ceram. Soc.*, 1999, **19**, 41–48.